PLOS ONE

RESEARCH ARTICLE

Platelet activation via dynamic conformational changes of von Willebrand factor under shear

Denis M. Pushin[1,2], Tatiana Y. Salikhova[2], Ksenia E. Zlobina[1], Georgy Th. Guria[1,2]*

1 National Research Center for Hematology, Moscow, Russia, **2** Moscow Institute of Physics and Technology, Dolgoprudny, Russia

* guria@blood.ru

Abstract

Shear-induced conformational changes of von Willebrand factor (VWF) play an important role in platelet activation. A novel approach describing VWF unfolding on the platelet surface under dynamic shear stress is proposed. Cumulative effect of dynamic shear on platelet activation via conformational changes of VWF is analysed. The critical condition of shear-induced platelet activation is formulated. The explicit expression for the threshold value of cumulative shear stress as a function of VWF multimer size is derived. The results open novel prospects for pharmacological regulation of shear-induced platelet activation through control of VWF multimers size distribution.

Introduction

It is known that high shear stresses induce platelet activation and subsequent aggregation [1–4]. This process is premised on the conformational unfolding of von Willebrand factor (VWF) molecules. Under certain shear flows, VWF multimers unfold, exposing more A1 domains capable of binding platelet receptors GPIb [5–9]. The initial activation of platelet signal cascades is triggered by the simultaneous coating of several GPIb receptors with A1 domains of a VWF molecule [10–12]. Multivalent binding of VWF molecules makes possible subsequent platelet aggregation. According to the current viewpoint, shear-induced platelet aggregation (SIPA) plays an important role in the development of myocardial infarction, stroke and some other diseases [13–16]. For that reason, SIPA has been intensively investigated *in vivo* and *in vitro* [17–19].

Under spatially uniform hydrodynamic conditions, *in vitro* platelet activation takes place at steady shear stress exceeding 80 (dyn/cm^2) [20–22]. In contrast, under unsteady conditions, particularly when blood moves in stenotic vessels, platelets can undergo high shear stress for only short time intervals [23]. Under such conditions, shear stress must act on platelets with VWF during a time interval sufficient for initial platelet activation. For this reason, it has been suggested that platelets become activated if the cumulative shear stress (CSS) is greater than a certain critical value (CSS_0) [24–27]:

$$CSS \equiv \int_{t_{in}}^{t_{out}} \tau(t)dt \geq CSS_0 \tag{1}$$

where $\tau(t)$ is the shear stress to which platelets are exposed under unsteady shear conditions at time t; t_{in} and t_{out} correspond to the time points when platelets move in and out of the high shear stress zone, respectively.

Data on the value of the threshold cumulative shear stress CSS_0 is highly controversial [28–34]. To the best of our knowledge, there has been no discussion of how the value of CSS_0 can depend on physicochemical properties of blood, including composition, degree of biomacro-molecule polymerization, etc.

In the current work, we propose an approach that allows us to analytically derive an expression for the condition of platelet activation under unsteady shear stress. The approach is based on the idea that under unsteady flow, the conformation of VWF molecules grafted on platelet surfaces can be dynamically changed. As a result of VWF unfolding, the efficient connection with multiple GPIb receptors on the platelet surface is increased. When the degree of connection is increased above a critical value, the platelet is assumed to be primed for activation. Under these assumptions, it was shown that platelet activation should truly take place if cumulative shear stress exceeds the definite threshold level. As a result of the proposed approach the dependence of the threshold value of cumulative shear stress as a function of the multimeric size of VWF molecules was derived.

Materials and methods

### Platelet activation in steady and unsteady shear flow

The unfolding of VWF macromolecules on the surface of platelets under steady shear stress was analysed previously [35]. It was established that the conformational state of VWF molecules adsorbed on the surface of platelets depends on the shear stress value. A bifurcation diagram displaying the dependence of the unfolding degree of VWF molecules on shear stress is shown in Fig 1.

The diagram shows that at low shear stress, $\tau < \tau_*$, there are two stable states of VWF molecules (folded and totally unfolded). If a VWF molecule is initially in globular form on the platelet surface when the shear stress starts to exceed the critical value τ_*, partial unfolding of the molecule should begin (branch BC). A further increase in shear stress leads to a second critical value τ_c, at which the partially unfolded state disappears as a result of fold catastrophe (point C). The system inevitably evolves to a completely unfolded state. From the bifurcation diagram (Fig 1), it is also clear that an unfolded state exists and is stable with respect to finite amplitude perturbation at all shear stress values either greater or less than τ_c (branch EF).

It also follows from the diagram that any partially unfolded state should return to the folded state during the gradual decline in shear stress τ (movement along the BC branch from point C to point B). This means that platelet activation by partially unfolded VWF molecules can take place only in the cases when the duration of overcritical shear stress is permanent or rather long [35].

Unlike partially unfolded states, VWF molecules in totally unfolded states remain resistant to any quasistatic changes in shear stress values. This means that if the VWF molecule was ever completely unfolded, it would remain in the completely unfolded state upon further increasing or decreasing the shear stress. In particular, if VWF molecules become completely unfolded as a result of platelets passing through stenotic regions of blood vessels containing high shear stress zones, molecules will continue to circulate in the blood in that completely unfolded state. Therefore, the exposure time of platelet GPIb receptors to VWF molecule action will not be limited by the time passing through the stenotic region.

In this paper, we investigate the conditions of VWF molecule total unfolding under the dynamic action of unsteady shear stress.
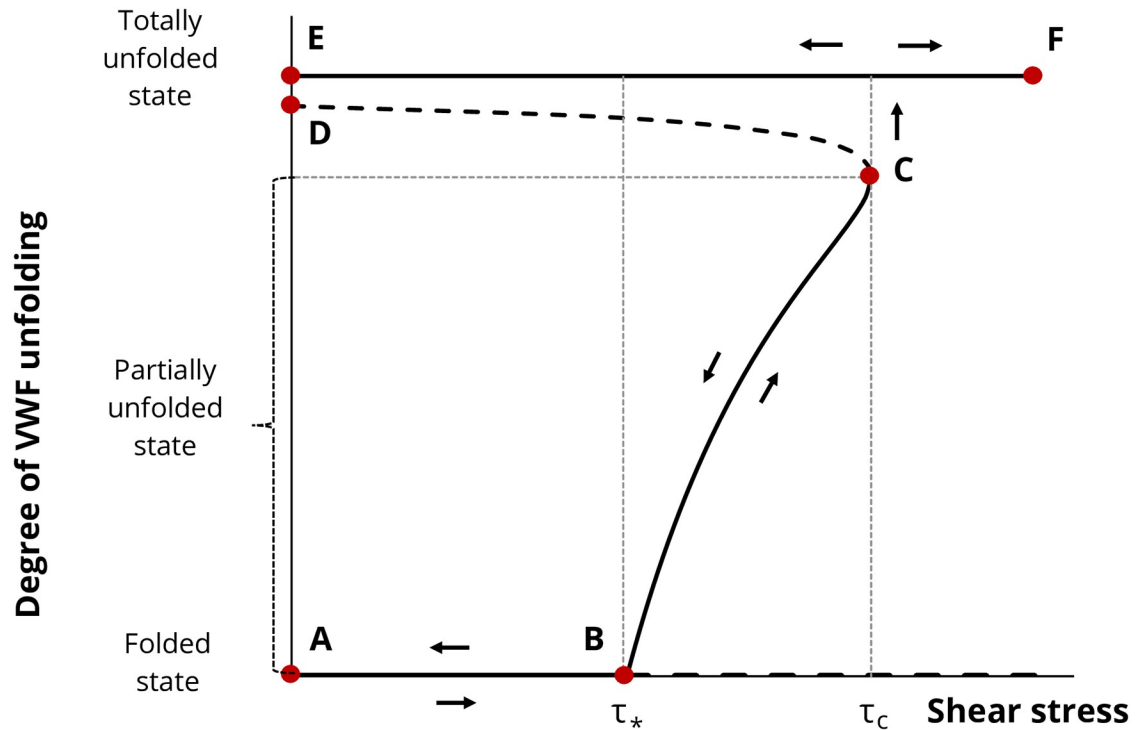
Fig 1. Bifurcation diagram of VWF conformational stability at different shear stresses. Bold lines display branches corresponding to stable steady states and dashed lines display branches corresponding to unstable steady states. τ_* is a bifurcation value of shear stress. The value τ_c is a value of shear stress under which VWF molecules must be unwound to their full length. Degree of unfolding (u) denotes a ratio of the tail length of the VWF molecule to the VWF contour length ($u = x/L$). Adapted from [35].

https://doi.org/10.1371/journal.pone.0234501.g001

VWF dynamics under unsteady shear stress

Consider a VWF molecule grafted at a definite point on a platelet surface. Assume that it consists of N subunits of size d each, where the VWF contour length is $L \equiv N \cdot d$. The molecule can be unfolded under shear stress acting on it in flow. Let the radius of the globular part of the molecule be denoted by r, while x denotes a length of the unfolded part of the molecule ("tail", Fig 2). The basic equation describing the VWF molecule dynamics on the platelet surface under unsteady shear stress may be written in accordance with the rules of analytical mechanics:

$$\frac{d}{dt}(J_r\omega) = M_{un} - M_f \tag{2}$$

where symbol J_r denotes the moment of inertia of the globular part of the VWF molecule and ω displays rotational speed of globular part of the molecule. $M_{un} \equiv F_{un}r$ is the moment of unfolding force F_{un} due to the action of shear stress on VWF molecules from the flow side, tending to unfold the molecule, and $M_f \equiv F_f r$ is the moment of folding force F_f, tending to return the molecule to a globular conformation.

Using a simple approximation [36,37], the unfolding force F_{un} can be evaluated as:

$$F_{un} = k\pi r^2 \tau \tag{3}$$

where $\tau = \tau(t)$ denotes the shear stress value and k represents a dimensionless proportionality coefficient. Folding force is caused by the presence of effective "surface tension" that tends to return a molecule to its most compact shape (globular state). The absolute value of the folding
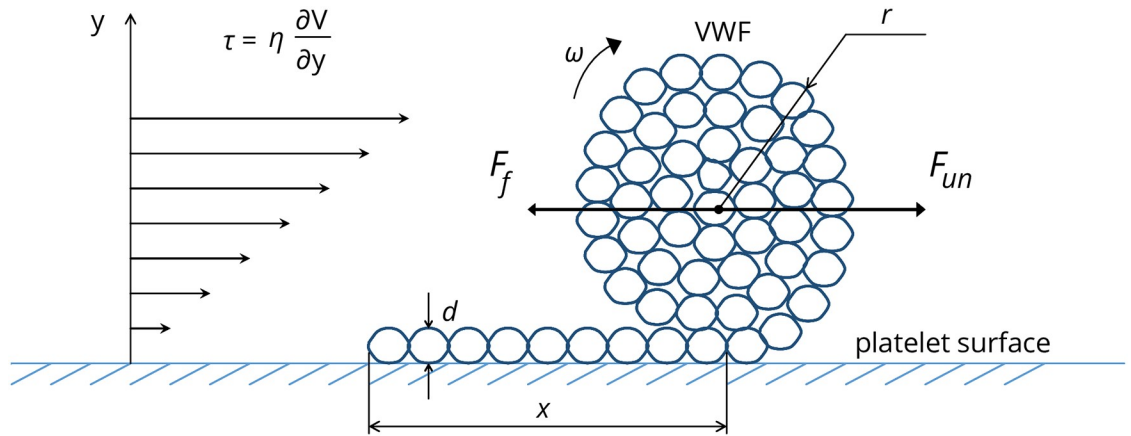
Fig 2. Partially unfolded VWF molecule in shear flow. r denotes the radius of the VWF globular part, x corresponds to the length of the unfolded part on the platelet surface ("tail") of the molecule, d denotes the characteristic size of the VWF monomeric subunit, F_f denotes the force due to effective surface tension that tends to fold a VWF molecule, F_{un} is the force that unfolds a VWF molecule under the action of shear stress τ, η denotes blood viscosity, and ω reflects the rotational speed of the globular part of the molecule. The symbol dV/dy denotes a velocity gradient perpendicular to the direction of the flow (i.e. shear rate). Adapted from [35].

https://doi.org/10.1371/journal.pone.0234501.g002

force is defined as follows (S1 Text):

$$F_f = \sigma\pi d\left(1 - \frac{d}{2r}\right) \tag{4}$$

where σ corresponds to the coefficient of the effective "surface tension".

Explicit expressions for the moment of inertia J_r and angular speed of the globular part of the molecule ω can be rewritten in the following forms (for details, S1 Text):

$$J_r = \frac{112r^5}{15d^3}m_0 \tag{5}$$

$$\omega = \frac{1}{r}\frac{dx}{dt} = -\frac{16r}{d^2}r'_t \tag{6}$$

The symbol m_0 in Eq (5) corresponds to the mass of a single monomeric subunit of the VWF molecule. Taking into account Eqs (3)–(6), the equation of motion (2), describing the conformational dynamics of the VWF macromolecule, can be easily transformed to the following form (S1 Text):

$$\frac{4m_0}{15\sigma\pi}\left[\left(\frac{2r}{d}\right)^7\right]''_{tt} = -\frac{k\tau d}{4\sigma}\left(\frac{2r}{d}\right)^3 + \left(\frac{2r}{d}\right) - 1 \tag{7}$$

where double prime denotes the second derivative of the expression with respect to time. Using the designation $q = (2r/d)^7$, the equation for VWF folding/unfolding (7) is converted to the following dimensionless form:

$$q''_{\tilde{t}\tilde{t}} = -\tilde{\tau}q^{3/7} + q^{1/7} - 1 \tag{8}$$

where $\tilde{t} \equiv t\sqrt{15\sigma\pi/4m_0}$ represents a dimensionless value, corresponding to time, while $\tilde{\tau} \equiv k\tau d/4\sigma$ denotes the dimensionless shear stress. Note that the dynamic dimensionless

variable $q \equiv q(\tilde{t})$ can vary from $q = q_m = (3N/2)^{7/3}$ (folded state) to $q = 0$ (totally unfolded state). One could receive the following relation between the order parameter $u = x/L$ and the variable q: $u = 1 - (q/q_m)^{3/7}$. Obviously, $u = 0$ if the VWF molecule is in its folded state, and $u = 1$ if VWF is in a totally unfolded state.

Eq (8) can be formally considered as a motion equation of a material point having a unit mass and coordinate q in a potential force field:

$$\tilde{U}\tilde{\tau}(q) = \frac{7}{10}\tilde{\tau}q^{10/7} - \frac{7}{8}q^{8/7} + q \qquad (9)$$

Note that the first term on the right-hand side of Eq (8) describes an action of shear stress $\tilde{\tau}$ and in principle can be time dependent (for instance, during platelet motion in vessels with a variable cross-section). The conformational states of molecules adsorbed on platelet surfaces will change in accordance with Eq (8) during platelet motion from low to high shear stress zones and back.

Results

Analysis of the phase portrait and formulation of the critical condition of shear-induced platelet activation

The central question is as follows: what are the conditions for irreversible conformational unfolding of VWF? Looking for the answer to this question, it seems appropriate to build phase portraits of the considered system in accordance with standard methods of analytical mechanics [38].

Profiles $\tilde{U}_{\tilde{\tau}}(q)$ corresponding to the potential energy drawn in accordance with Eq (9) are shown in Fig 3. The potential energy curves for the three sets of $\tilde{\tau}$ values have different numbers of extrema.

When the value of shear stress satisfies the condition $\tilde{\tau} > \tilde{\tau}_c$, all the corresponding curves of potential energy have only one minimum at $q = 0$ (Fig 3, red region). This means that in quite intense steady shear flows, VWF molecules should be in totally unfolded states. The second possibility is realized when $\tilde{\tau}_* < \tilde{\tau} < \tilde{\tau}_c$ (yellow region). In this region, all curves of potential energy have two local minima: one at $q = 0$ and the other at $q = q_c$ belonging to the region (q_s, q_m). This means that VWF molecules should be either in the completely unfolded state ($q = 0$) or in a partially unfolded state ($q = q_c$). Finally, when $\tilde{\tau} < \tilde{\tau}_*$ (green region), the curves of potential energy have two local minima: one at $q = 0$ and the other at $q = q_m$. In relevant flows, VWF molecules should be either in the completely unfolded state ($q = 0$) or in the folded state ($q = q_m$). It should be noted that under the condition $\tilde{\tau} < \tilde{\tau}_c$, every curve of potential energy also has one local maximum at $q = q_s$.

It is clear that potential energy minima correspond to the states in which the dynamic system has a tendency to remain if left to itself. A local maximum of potential energy defines the height of a barrier that the system needs to overcome for transition from one local stable state ($q = q_m$) to another ($q = 0$).

The phase portrait of the system for the case $\tilde{\tau} = 0$ is shown in Fig 4 (topological transformations of phase portraits for abovementioned intervals of shear stress $\tilde{\tau} > 0$ are shown in S2-1 Fig, S2 Text). It is clear that to change the molecular conformation from the initially folded state $q = q_m$, $\dot{q} = 0$ (point D) to the totally unfolded state $q = 0$, the momentum imparted to the molecule must be rather strong. The corresponding image point, representing the system state, should fall at a definite moment below the separatrix AS (shown in Fig 4 by a bold line).

One of the possible ways to impart the momentum $\dot{q}$ to the molecule is to expose it to shear stress. Let us consider the response of the VWF molecule to a rectangular shear stress impulse
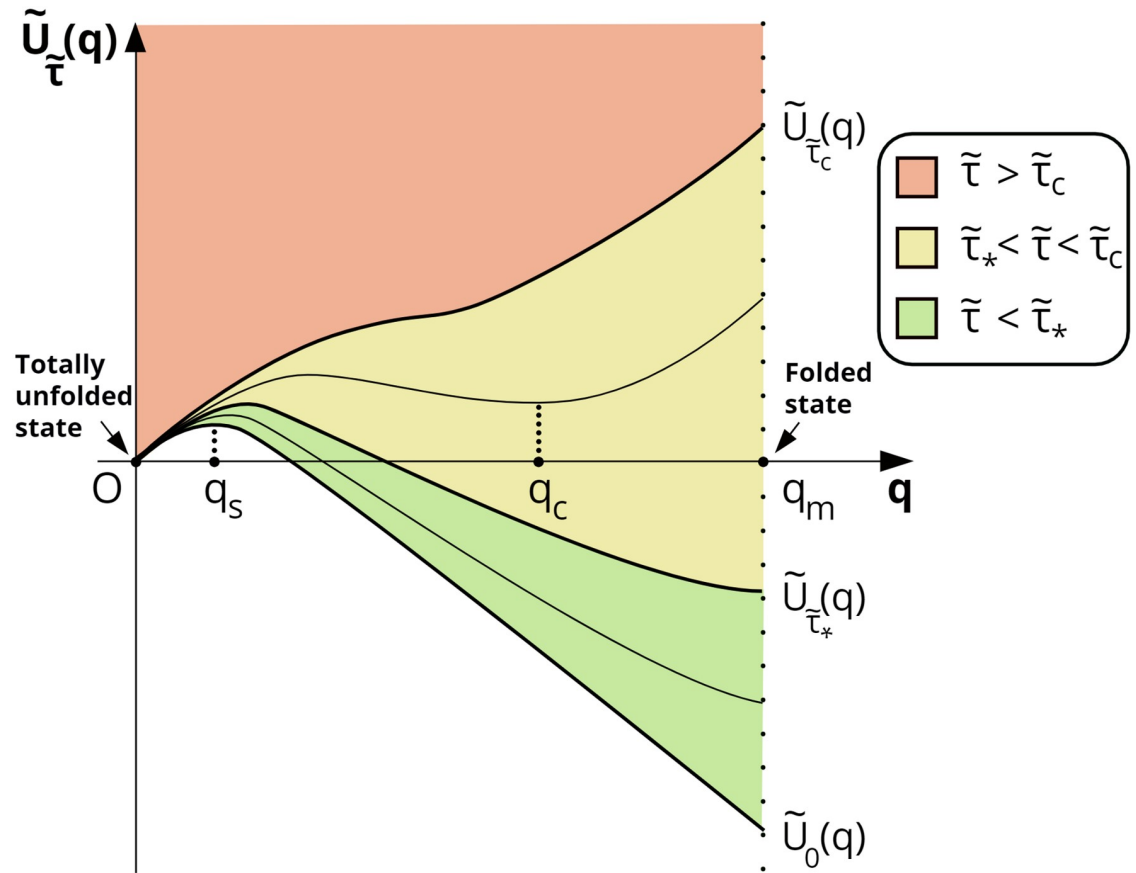
Fig 3. Potential energy profile $\tilde{U}_{\tilde{\tau}}(q)$ at various $\tilde{\tau}$ values. Three characteristic regions are shown. Any potential curve at $\tilde{\tau} > \tilde{\tau}_c$, $\tilde{\tau}_* < \tilde{\tau} < \tilde{\tau}_c$ and $\tilde{\tau} < \tilde{\tau}_*$ lies in the domain denoted in red, yellow and green, respectively. Points $q = q_s$ and $q = q_c$ are points of maximum and minimum potential energy $\tilde{U}_{\tilde{\tau}}(q)$, respectively. Bold lines correspond to potential energy curves for $\tilde{\tau} = 0$, $\tilde{\tau} = \tilde{\tau}_*$, and $\tilde{\tau} = \tilde{\tau}_c$ and are define as $\tilde{U}_0(q)$, $\tilde{U}_{\tilde{\tau}_*}(q)$ and $\tilde{U}_{\tilde{\tau}_c}(q)$, respectively.

(Fig 5). After application of a rectangular shear stress impulse of amplitude $\tilde{\tau}_m$ and duration $\tilde{t}_G$ (Fig 5a), the phase trajectory starting from point D crosses the separatrix AS (Fig 5b) at a certain moment $\tilde{t}_F$. All integral curves passing below the separatrix AS (Fig 5b) reach the left boundary of the physically acceptable region ($q = 0$) below point B. That is, all these curves lead to the completely unfolded state of VWF molecules on the platelet surface. Clearly, VWF molecules that go to the unfolded state ($q = 0$) will have nonzero momentum $|\dot{q}| > |\dot{q}_B| \neq 0$ at the time of their complete unfolding to $q = 0$. Moreover, the lower the situated corresponding integral curve at the phase portrait, the larger the absolute value of the "residual" momentum.

Further evolution of the unfolded VWF molecule depends on the boundary conditions at $q = 0$. In principle, there are three possibilities depending on the particularities of platelet surface interaction with VWF molecules (all possibilities mentioned above are discussed in detail in S2 Text): absolutely inelastic, partially elastic and absolutely elastic collision. The absolutely elastic boundary condition corresponds to the situation when there is no energy loss in a collision. VWF multimer being totally unfolded retains an opportunity to return back to its initial folded state in this case. The absolutely inelastic boundary condition corresponds to irreversible adhesion of VWF molecules on the platelet surface after unfolding. We suppose that some
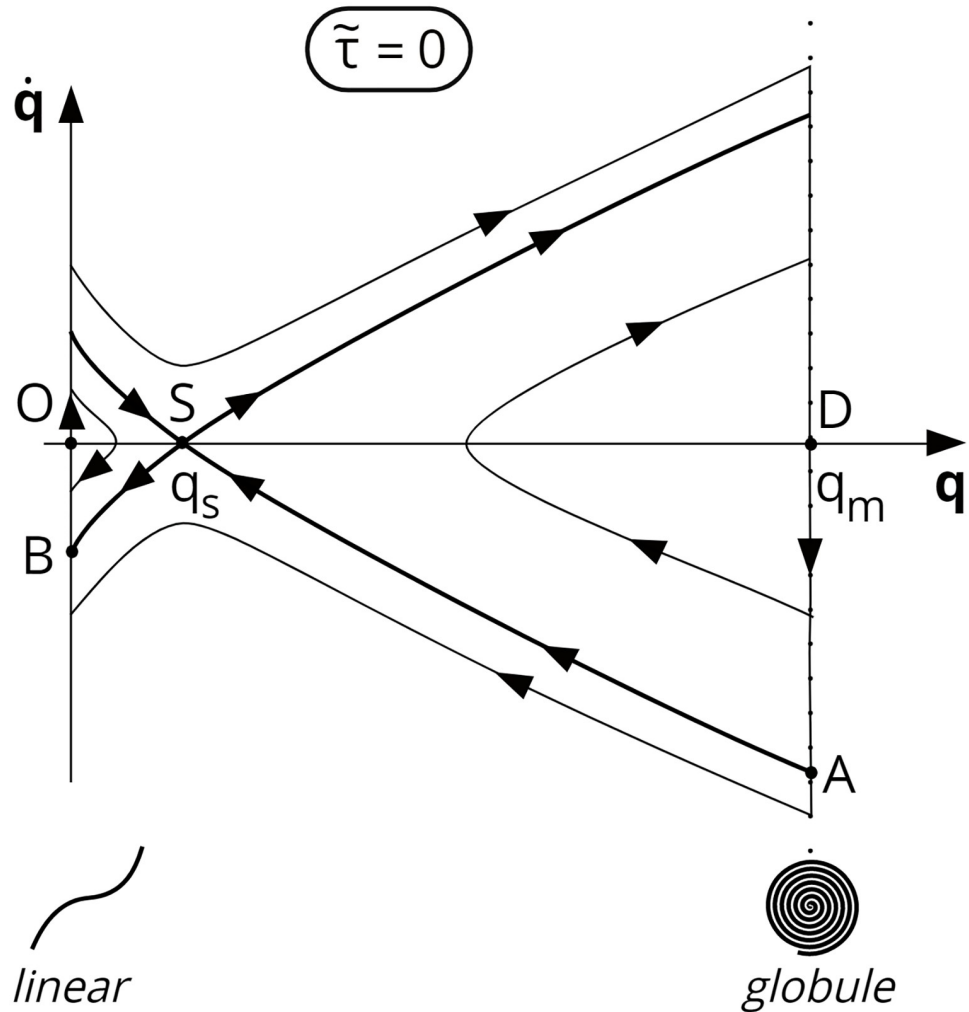
Fig 4. Schematic view of the phase portrait at $\tilde{\tau} = 0$. The value $q = 0$ corresponds to the unfolded state of the VWF molecule; and $q = q_m$, to the folded state. $q = q_s$ is a saddle point, and the curve ASB denotes the separatrix.

intermediate situation takes place in a real situation corresponding to a partially elastic boundary (see S2 Text for details).

Numerical investigation of the critical cumulative shear stress condition achieved for the case of a rectangular shear impulse is discussed in detail in S4 Text. In particular, the dependence of $\tilde{t}_F$ on the value of applied shear stress $\tilde{\tau}_m$ (for any definite value of N) was found (Fig 6).

The dependence $\tilde{t}_F(\tilde{\tau}_m)$ is shown in Fig 6. It has a vertical asymptote $\tilde{\tau}_m = \tilde{\tau}_{\#}$. At the same time, it is clear that within a fairly wide range of amplitudes $\tilde{\tau}_m (\tilde{\tau}_m > 2\tilde{\tau}_c)$, the curve may be approximated by the expression $\tilde{\tau}_m \tilde{t}_F = CSS_0$. The value of CSS_0 is determined by Eq (16). The dependence of $\tilde{\tau}_{\#}$ as a function of N is given in S4-3 Fig (S4 Text).

Indeed, it is easily seen from Fig 6 that the solid line (reflecting rigorous condition of VWF unfolding) lies above the dashed line relevant to the curve $\tilde{\tau}_m \tilde{t}_F = CSS_0$. Thus, condition $\tilde{\tau}_m \tilde{t}_F > CSS_0$ should be treated as the necessary condition, while the rigorous sufficient condition is determined by the numerical solution to Eq (8) represented by the solid line in Fig 6.
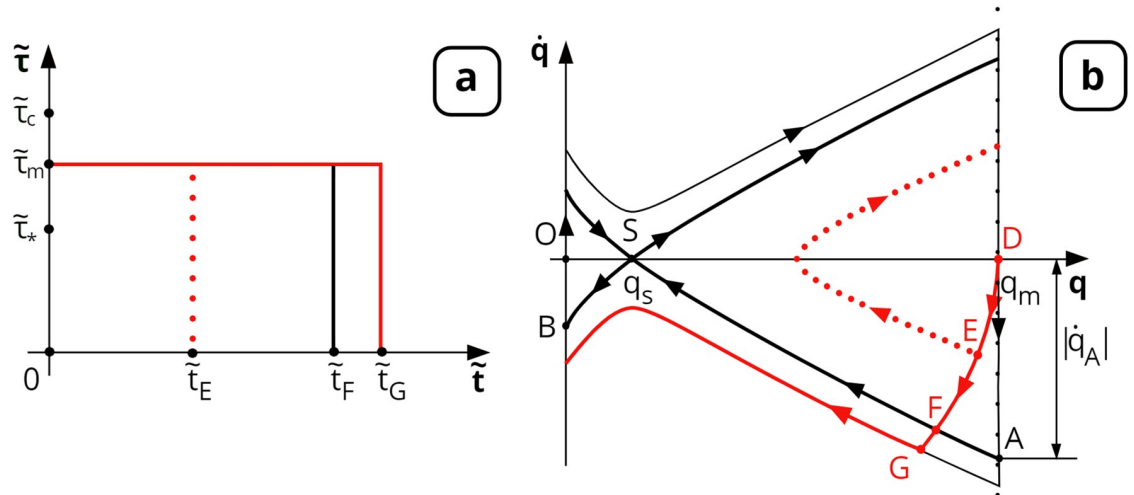
Fig 5. VWF molecule unfolding under the action of a rectangular shear stress profile with various durations. (a) Shear stress impulse $\tilde{\tau}(\tilde{t})$ is shown in red, $\tilde{\tau}_m$ is its amplitude, and $\tilde{t}_G$ is its duration. (b) Phase trajectory of the solution (Eq (8)) is illustrated by the red line for the shear stress profile from Fig 5a; initial conditions: $q = q_m$, $\dot{q} = 0$. $\tilde{t}_E$, $\tilde{t}_F$ and $\tilde{t}_G$ are time moments when the image point reaches points E, F and G, respectively. If the duration of the shear stress impulse $\tilde{t}_G$ is greater than that of $\tilde{t}_F$, the trajectory crosses the part of the separatrix AS, and the molecule can unwind to its full length. $|\dot{q}_A|$ is the absolute value of the momentum at point A.

The two lines practically coincide with each other when $\tilde{\tau}_m > 2\tilde{\tau}_c$. However, in the interval $\tilde{\tau}_m \in (\tilde{\tau}_*, 2\tilde{\tau}_c)$, the discrepancy between the lines is significant. Moreover, it can be seen from Fig 6 that total unfolding of VWF induced by a shear stress less than the threshold value $\tilde{\tau}_m < \tilde{\tau}_*$ is not possible at any finite time interval. Thus, relevant platelet activation should not take place.

Derivation of the explicit expression for the CSS_0 as a function of VWF multimer size

It is worth to notice that the approach developed in the current work makes it possible to investigate VWF unfolding and relevant platelet activation not only for a rectangular profile of shear stress but also for an arbitrary form of shear stress $\tau(t)$ as a function of time. Indeed, below, we demonstrate analytically how the critical condition for cumulative shear stress can be derived.

Consider a VWF molecule passing through a high shear stress zone. $\dot{q}_{in}$ and $\dot{q}_{out}$ correspond to momentum at moments $\tilde{t}_{in}$ and $\tilde{t}_{out}$, respectively, when platelets go in and out of the high shear stress zone. Suppose that the VWF molecule is in a folded state at the initial moment $\tilde{t}_{in}$. That formally means that $q(\tilde{t}_{in}) = q_m$ and $\dot{q}_{in} \equiv \dot{q}(\tilde{t}_{in}) = 0$. Looking at the phase portrait (Fig 5b), it becomes clear that the sufficient condition of total VWF unfolding has the form:

$$|\dot{q}_{out}| > |\dot{q}_A| \tag{10}$$

It is easy to obtain the value of the momentum at point A (S3 Text):

$$|\dot{q}_A| = \sqrt{2(\tilde{U}_0(q_s) - \tilde{U}_0(q_m))} \tag{11}$$
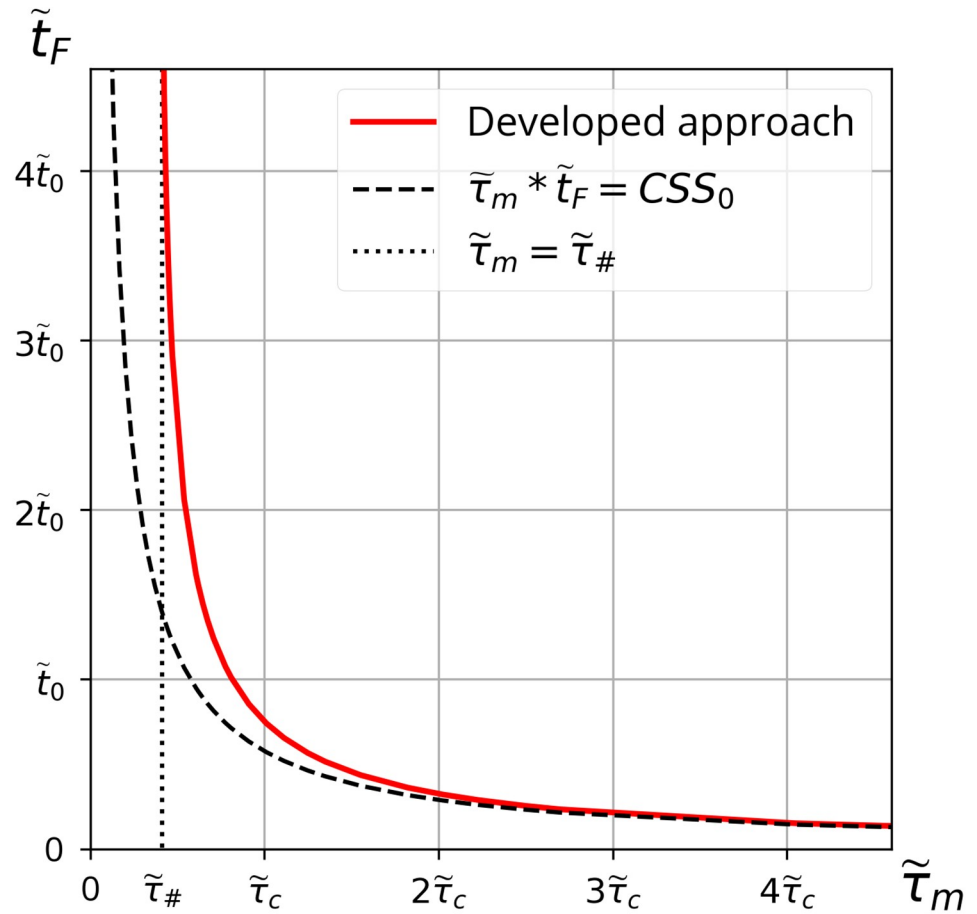
Fig 6. Dependence of critical time duration $\tilde{t}_F$ on amplitude $\tilde{\tau}_m$ of a rectangular shear stress impulse. The solid curve corresponds to the dependence $\tilde{t}_F(\tilde{\tau}_m)$ obtained in the framework of developed approach (S4 Text for details). The dotted line $\tilde{\tau}_m = \tilde{\tau}_\#$ is a vertical asymptote of the curve $\tilde{t}_F(\tilde{\tau}_m)$. The curve $\tilde{t}_F(\tilde{\tau}_m)$ is asymptotically tending to the dashed curve with increasing $\tilde{\tau}_m$. The values of $\tilde{t}_F$ are measured in units of characteristic unfolding time $\tilde{t}_0$ (S4 Text). The value of CSS_0 is given by Eq (16). All curves were built for the case of $N = 36$.

The momentum value $\dot{q}_{out}$, that a VWF molecule obtained when passing through the high shear stress zone, can be found by integrating Eq (8) with respect to time:

$$\dot{q}_{out} - \dot{q}_{in} = \int_{\tilde{t}_{in}}^{\tilde{t}_{out}} \hat{A}\dot{q}\,d\tilde{t} = \int_{\tilde{t}_{in}}^{\tilde{t}_{out}} \left(-\tilde{\tau}q^{\frac{3}{7}} + q^{\frac{1}{7}} - 1\right)d\tilde{t} \qquad (12)$$

Taking into account that $\dot{q}_{in} = 0$, Eq (12) can be transformed into the following form:

$$|\dot{q}_{out}| = \int_{\tilde{t}_{in}}^{\tilde{t}_{out}} q^{\frac{3}{7}}\tilde{\tau}(\tilde{t})\,d\tilde{t} - \int_{\tilde{t}_{in}}^{\tilde{t}_{out}} \left(q^{\frac{1}{7}} - 1\right)d\tilde{t} \qquad (13)$$

By substituting Eqs (11) and (13) into inequality (10) and keeping in mind that $q > q_s = 1$ under $\tilde{\tau} = 0$ the necessary condition for complete VWF unfolding takes the form (for details

S3 Text):

$$\int_{\tilde{t}_{in}}^{\tilde{t}_{out}} q^{\frac{3}{7}}\tilde{\tau}(\tilde{t})d\tilde{t} > \sqrt{2(\tilde{U}_0(q_s) - \tilde{U}_0(q_m))}$$ (14)

Taking into account that the values of the dynamical variable $q(t)$ during VWF unfolding are always less than its maximal value q_m ($q(t) < q_m$) the following inequality can be obtained:

$$\int_{\tilde{t}_{in}}^{\tilde{t}_{out}} \tilde{\tau}(\tilde{t})d\tilde{t} > \frac{1}{q_m^{\frac{3}{7}}} \sqrt{2[\tilde{U}_0(q_s) - \tilde{U}_0(q_m)]} \equiv CSS_0$$ (15)

In other words, to unfold a VWF multimer, the value of the cumulative shear stress must be at least larger than a definite critical value CSS_0 standing on the right-hand side of inequality (15). Expression (15) represents the necessary but not sufficient condition of VWF unfolding on the surface of platelets.

The developed approach gives us the opportunity not only to find an expression for the condition of the cumulative shear stress (Eq (15)) but also to find the dependence of CSS_0 as a function of N. Indeed, taking into consideration that $q_s = 1$, $q_m = (3N/2)^{7/3}$ and that the expression for potential energy has a form $\tilde{U}_0(q) = -(7/8)q^{8/7} + q$, the value of the critical cumulative shear stress is given by the following formula:

$$CSS_0 = \left(\frac{3}{2}N\right)^{\frac{1}{3}} \sqrt{\frac{7}{4} + \frac{1}{4}\left(\frac{3}{2}N\right)^{-\frac{8}{3}} - 2\left(\frac{3}{2}N\right)^{-\frac{1}{3}}}$$ (16)

Eq (16) represents an explicit expression for the dependence of the critical cumulative shear stress CSS_0 value on the multimeric size of VWF molecules. Thus, the value of the critical cumulative shear stress is an increasing function of the VWF multimer size N.

Discussion

In the current work, we propose an approach for the analytical derivation of the platelet activation conditions under unsteady shear stress (expressions (15) and (16)). The approach is based on the idea that the conformation of VWF molecules which are grafted on platelet surfaces can be dynamically changed under unsteady flow. VWF unfolding results in the increase of an efficient connection between VWF monomer units and GPIb receptors on the platelet surface. When the cumulative shear stress exceeds a critical value (inequality (15)), the platelet is primed for activation. As a result of the proposed approach, the dependence of the threshold value of cumulative shear stress on VWF multimer size was derived (Eq (16)).

The problem of shear-induced unfolding of VWF molecules and its presumable effect on platelet activation has been intensively studied during the last four decades [21,39–41]. Most of the previous studies focused on the investigation of VWF-platelet interactions under steady shear stress. Particularly, the platelet activation was analysed in microcirculation [18,42]. In contrast, in stenotic regions of large vessels platelets are exposed to unsteady shear stress, rapidly varying along platelet trajectories. For this reason, in the present article we focused on the investigation of unsteady shear-induced platelet activation (SIPAct) phenomena in large vessels.

Shear gradients, as well as the duration of exposure to high shear stress, can influence the onset of SIPAct in the presence of VWF molecules [18,28,31,34,43,44]. The haemostatic activity of VWF directly correlates with its size [39,45]. To the best of our knowledge, no mathematical expression describing SIPAct relation to the characteristics of dynamic shear stress

(amplitude and duration) and the length of VWF molecules has been suggested. Corresponding formulas are derived in this work (Eqs (15) and (16)).

The approach allowed us to derive the equation for VWF folding/unfolding on a platelet surface under dynamic shear stress. It was shown that conformational changes of VWF during platelet movement through a high shear stress zone can be calculated by numerical integration of Eq (8). This equation may be used for the estimation of shear-induced platelet activation under unsteady flow conditions. Particularly, basing on Eq (8), condition (15) for complete VWF unfolding on the platelet surface under dynamic shear was obtained. According to this condition, any value of cumulative shear stress less than the threshold value should not lead to full unfolding of VWF.

The analytical expression for the critical cumulative shear stress as a function of VWF multimer size (Eq (16)) was derived. When passing through a high shear zone, VWF experiences an "impact" that may lead to full unfolding. Eq (16) shows that large multimers need stronger "impact" for full unfolding than smaller multimers.

The unfolding of VWF under the action of a rectangular shear stress profile was investigated numerically (Fig 5). The obtained results indicate that in the case of short but rather strong shear impulses ($\tilde{\tau}_m > 2\tilde{\tau}_c$), condition (15) may be used as a high accuracy approximation for the condition of full unfolding of VWF on the platelet surface, resulting in subsequent priming of the platelet (Fig 6).

Condition (15) is suitable for describing shear-induced platelet activation in laminar blood flow. In such a flow, it is always possible to distinguish trajectories of individual platelets and to track how shear stress is changing along trajectories. The finding of dependencies of shear stress along a trajectory in laminar flow seems to be a standard computational fluid dynamics (CFD) task [46]. In particular, this task can be routinely solved for blood vessels with variable cross-sections [24,25]. Once the dependency is obtained, one can easily check the fulfilment of condition (15) for any selected platelet trajectory.

The applicability of the developed approach to the investigation of shear-induced platelet activation in turbulent blood flow remains unclear and requires further study.

In further analysis of laminar blood flow, it is worth taking into account that hydrodynamic conditions corresponding to shear-induced platelet activation may be divided into two groups [47–50]. The first group includes situations where shear stress is steady (for instance, as in a cone-and-plate viscometer) and exposure time lies within the range from several seconds to minutes [39,40,47]. The second group includes regimes in locally stenotic blood vessels *in vivo* and constricted artificial channels *in vitro*. The current experimental data show that the characteristic time during which platelets are exposed to high shear stress varies from a few milliseconds to fractions of seconds [23,51], while the characteristic amplitude of shear stress may exceed 1000 (*dyn*/*cm*^{2}) [52,53].

According to the approach developed in this paper, the difference between the two groups is related to the value of the shear stress gradient, i.e., the derivative of $\tilde{\tau} = \tilde{\tau}(\tilde{t})$. In cases where the shear stress gradient is sufficiently small, the shear stress along the platelet trajectory will vary more slowly than the conformation of the VWF molecule. Thus, the value of shear stress could be considered a parameter in Eq (8). Platelet activation under such conditions takes place in a parametric regime. In cases where the shear stress gradient is sufficiently large, VWF conformational changes will delay after shear stress variations. In other words, rapid platelet movements through the stenotic region result in an impulsive hydrodynamic impact on VWF. Under impulsive impacts, the shear stress in Eq (8) could be treated as a dynamical variable. Therefore, SIPAct under such conditions occurs in a dynamic regime.

The corresponding momentum acquired by the VWF may be subcritical (less than $|\dot{q}_A|$) or overcritical (more than $|\dot{q}_A|$)). In the second case, such momentum is enough for full unfolding of VWF on the platelet surface (Fig 5). The relevant condition (10) formally may be considered a sufficient condition for the total unfolding of VWF, which seems to be a necessary condition for the priming of platelets.

The developed approach allows us to analyse both the impulsive and quasistatic evolution of the VWF conformation on the platelet surface. In the case of impulsive evolution, one could say that the hydrodynamic environment around platelets changes faster than the conformation of VWF molecules on their surface. On the other hand, when quasistatic evolution takes place, VWF molecules can adapt their conformations under external actions. The degree of their unfolding follows the changes in shear stress. The conformational state of VWF may be established from the equilibrium conditions derived from Eq (8).

In cases where shear stress impacts act during a very short period of time, VWF should relax to new equilibrium states over some period of time. In the current work, our purpose was limited only to an estimation of phase portrait transformations corresponding to the dynamics of the VWF molecule to equilibrium states under small dissipative effects (S2 Text).

It is well known that shear stress reaches the highest values in the near-wall region of vessels [54] The concept of wall shear stress (WSS) has become widespread not only among CFD specialists but also among physicians [55,56]. To interpret the results obtained in this paper, it should be noted that the velocity of platelets moving near the vessel wall tends to zero under no-slip conditions [57]. For all trajectories lying adjacent to the vessel wall, dependencies of shear stress are slowly varying functions of time. This means that the conditions for VWF unfolding in near-wall regions can be considered parametric.

The farther from the wall the trajectory of motion is, the shorter the time it takes for a platelet to cross through a locally stenotic region. Thus, short-term impulsive action from the side of the flow on VWF molecules should take place. The question is whether this kind of impulsive action may lead to full unfolding of VWF on platelet surfaces resulting in subsequent priming of the platelets. The answer is given by condition (15) obtained in this paper. Consequently, within the framework of our approach, both parametric and dynamic regimes of SIPAct can simultaneously be realized in the same stenotic artery but at a different distance from the vessel wall.

It is worth discussing the extent to which the obtained results may be relevant to problems of thrombosis initiation in different blood-wetted devices. For the moment, we can formulate a few conclusions concerning cumulative shear stress. At high shear stress ($\tilde{\tau}_m > 2\tilde{\tau}_c$), approximation condition (1) is quite suitable for the estimation of device thrombogenicity. When the shear stress lies in the range of $\tilde{\tau}_\# < \tilde{\tau}_m < 2\tilde{\tau}_c$, condition (1) could be treated as necessary but insufficient for SIPAct. If the shear stress is less than the threshold level $\tilde{\tau}_m < \tilde{\tau}_\#$, condition (1) is unusable for the evaluation of platelet activation.

The existence of a lower shear stress threshold above which SIPAct may take place is intensively discussed in some articles dedicated to the problem of thrombogenicity in blood-wetted devices [58,59] and in stenotic vessels [25,31]. The obtained results give the answer as to how the value of the lower threshold should depend on the multimeric size N of VWF molecules (S4-3 Fig of S4 Text).

Several experiments were conducted to study platelet function under high shear stress in different microfluidic platforms [17,18,22,43,60,61]. Particularly, the influence of dynamic shear stress on platelet activation was investigated [28,34,42]. We think that a critical value of cumulative shear stress as a function of multimer size could be measured in the framework of the microfluidic experiments. The regulation of the size of VWF molecules in relevant experimental conditions may be fulfilled with the aid of ADAMTS-13 [4,62,63]. Appropriate

experiments in large-scale vessels also could be done. It will give an opportunity for the direct confirmation/falsification of our theoretical results.

It is worth noting that in general, the developed approach is phenomenological. It describes the SIPAct phenomena under unsteady shear stress rather roughly, in contrast to the detailed molecular dynamics approach [64,65]. Nevertheless, the developed approach opens the possibility for estimating the relative impact of parametric and dynamic regimes of VWF unfolding on shear-induced platelet activation in a variety of arterial and venous vessels of the human blood circulatory system. Indeed, an explicit formula for the critical cumulative shear stress as a function of VWF multimer size is found (Eq (16)). This expression is important for the regulation of shear-induced platelet activation not only by biomechanical factors (WSS, arterial pressure, distensibility of vessel walls, etc.) [19,66], but also by several biochemical and pharmacological agents affecting VWF multimer size (ADAMTS-13, N-acetylcysteine) [4,67–69].

We believe that these findings may be used to improve clinical protocols for haemostasis correction.

Supporting information

S1 Text. Derivation of the dynamic VWF unfolding equation.
(PDF)

S2 Text. Analysis of solution behaviour at physical boundaries.
(PDF)

S3 Text. Derivation of the critical condition of the total VWF unfolding.
(PDF)

S4 Text. VWF unwinding under the action of rectangular shear stress profile.
(PDF)

Acknowledgments

Author Contributions

Conceptualization: Ksenia E. Zlobina, Georgy Th. Guria.

Formal analysis: Denis M. Pushin, Tatiana Y. Salikhova, Ksenia E. Zlobina, Georgy Th. Guria.

Methodology: Denis M. Pushin, Tatiana Y. Salikhova, Ksenia E. Zlobina, Georgy Th. Guria.

Software: Denis M. Pushin.

Supervision: Georgy Th. Guria.

Visualization: Tatiana Y. Salikhova, Ksenia E. Zlobina.

Writing – original draft: Denis M. Pushin.

Writing – review & editing: Denis M. Pushin, Tatiana Y. Salikhova, Ksenia E. Zlobina, Georgy Th. Guria.

References

1. O'Brien JR. Shear-induced platelet aggregation. The Lancet. 1990; 335(8691):711–3.

2. Kroll MH, Hellums JD, McIntire LV, Schafer AI, Moake JL. Platelets and shear stress. Blood. 1996; 88 (5):1525–41. PMID: 8781407

3. Sakariassen KS, Orning L, Turitto VT. The impact of blood shear rate on arterial thrombus formation. Future Sci. OA. 2015; 1(4):FSO30. https://doi.org/10.4155/fso.15.28 PMID: 28031903

4. Rana A, Westein E, Niego B, Hagemeyer CE. Shear-dependent platelet aggregation: mechanisms and therapeutic opportunities. Front. Cardiovasc. Med. 2019; 6:141. https://doi.org/10.3389/fcvm.2019.00141 PMID: 31620451

5. Siediecki CA, Lestini BJ, Kottke-Marchant KK, Eppell SJ, Wilson DL, Marchant RE. Shear-dependent changes in the three-dimensional structure of human von Willebrand factor. Blood. 1996; 88(8):2939–50. PMID: 8874190

6. Schneider SW, Nuschele S, Wixforth A, Gorzelanny C, Alexander-Katz A, Netz RR, et al. Shear-induced unfolding triggers adhesion of von Willebrand factor fibers. Proc. Natl. Acad. Sci. USA. 2007; 104(19):7899–903. https://doi.org/10.1073/pnas.0608422104 PMID: 17470810

7. Singh I, Themistou E, Porcar L, Neelamegham S. Fluid shear induces conformation change in human blood protein von Willebrand factor in solution. Biophys. J. 2009; 96(6):2313–20. https://doi.org/10.1016/j.bpj.2008.12.3900 PMID: 19289057

8. Fu H, Jiang Y, Yang D, Scheiflinger F, Wong WP, Springer TA. Flow-induced elongation of von Willebrand factor precedes tension-dependent activation. Nat. Commun. 2017; 8(1):324. https://doi.org/10.1038/s41467-017-00230-2 PMID: 28831047

9. Wang Y, Morabito M, Zhang XF, Webb E III, Oztekin A, Cheng X. Shear-induced extensional response behaviors of tethered von Willebrand factor. Biophys. J. 2019; 116(11):2092–102. https://doi.org/10.1016/j.bpj.2019.04.025 PMID: 31103230

10. Andrews RK, López J, Berndt MC. Molecular mechanisms of platelet adhesion and activation. Int. J. Biochem. Cell. Biol. 1997; 29(1):91–105. https://doi.org/10.1016/s1357-2725(96)00122-7 PMID: 9076944

11. Kasirer-Friede A, Ware J, Leng L, Marchese P, Ruggeri ZM, Shattil SJ. Lateral clustering of platelet GP Ib-IX complexes leads to up-regulation of the adhesive function of integrin αIIbβ3. J. Biol. Chem. 2002; 277(14):11949–56. https://doi.org/10.1074/jbc.M108727200 PMID: 11812775

12. Mody NA, King MR. Platelet adhesive dynamics. Part II: high shear-induced transient aggregation via GPIbα-vWF-GPIbα bridging. Biophys. J. 2008; 95(5):2556–74. https://doi.org/10.1529/biophysj.107.128520 PMID: 18515386

13. Konstantopoulos K, Grotta JC, Sills C, Wu KK, Heliums JD. Shear-induced platelet aggregation in normal subjects and stroke patients. Thromb. Haemost. 1995; 74(5):1329–34. PMID: 8607118

14. Goto S, Sakai H, Goto M, Ono M, Ikeda Y, Handa S, et al. Enhanced shear-induced platelet aggregation in acute myocardial infarction. Circulation. 1999; 99(5):608–13. https://doi.org/10.1161/01.cir.99.5.608 PMID: 9950656

15. Ajzenberg N, Aubry P, Huisse MG, Cachier A, El Amara W, Feldman LJ, et al. Enhanced shear-induced platelet aggregation in patients who experience subacute stent thrombosis: a case-control study. J. Am. Coll. Cardiol. 2005; 45(11):1753–6. https://doi.org/10.1016/j.jacc.2004.10.079 PMID: 15936600

16. Spiel AO, Gilbert JC, Jilma B. von Willebrand factor in cardiovascular disease: focus on acute coronary syndromes. Circulation. 2008; 117(11):1449–59. https://doi.org/10.1161/CIRCULATIONAHA.107.722827 PMID: 18347221

17. Nesbitt WS, Westein E, Tovar-Lopez FJ, Tolouei E, Mitchell A, Fu J, et al. A shear gradient–dependent platelet aggregation mechanism drives thrombus formation. Nat. Med. 2009; 15(6):665–73. https://doi.org/10.1038/nm.1955 PMID: 19465929

18. Jain A, Graveline A, Waterhouse A, Vernet A, Flaumenhaft R, Ingber DE. A shear gradient-activated microfluidic device for automated monitoring of whole blood haemostasis and platelet function. Nat. Commun. 2016; 7(1):10176. https://doi.org/10.1038/ncomms10176 PMID: 26733371

19. Chiu WC, Tran PL, Khalpey Z, Lee E, Woo YR, Slepian MJ, et al. Device thrombogenicity emulation: an in silico predictor of on vitro and in vivo ventricular assist device thrombogenicity. Sci. Rep. 2019; 9 (1):2946. https://doi.org/10.1038/s41598-019-39897-6 PMID: 30814674

20. Miyazaki Y, Nomura S, Miyake T, Kagawa H, Kitada C, Taniguchi H, et al. High shear stress can initiate both platelet aggregation and shedding of procoagulant containing microparticles. Blood. 1996; 88 (9),3456–64. PMID: 8896411

21. Shankaran H, Alexandridis P, Neelamegham S. Aspects of hydrodynamic shear regulating shear-induced platelet activation and self-association of von Willebrand factor in suspension. Blood. 2003; 101(7):2637–45. https://doi.org/10.1182/blood-2002-05-1550 PMID: 12456504

22. Lee H, Kim G, Lim C, Lee B, Shin S. A simple method for activating the platelets used in microfluidic platelet aggregation tests: Stirring-induced platelet activation. Biomicrofluidics. 2016; 10(6):064118. https://doi.org/10.1063/1.4972077 PMID: 28058084

23. Wurzinger LJ, Opitz R, Blasberg P, Schmid-Schönbein H. Platelet and coagulation parameters following millisecond exposure to laminar shear stress. Thromb. Haemost. 1985; 54(2):381–6. PMID: 2934855

24. Bluestein D, Niu L, Schoephoerster RT, Dewanjee MK. Fluid mechanics of arterial stenosis: relationship to the development of mural thrombus. Ann. Biomed. Eng. 1997; 25(2):344–56. https://doi.org/10.1007/BF02648048 PMID: 9084839

25. Tambasco M, Steinman DA. Path-dependent hemodynamics of the stenosed carotid bifurcation. Ann. Biomed. Eng. 2003; 31(9):1054–65. https://doi.org/10.1114/1.1603257 PMID: 14582608

26. Bark DL Jr, Ku DN. Wall shear over high degree stenoses pertinent to atherothrombosis. J. Biomech. 2010; 43(15):2970–7. https://doi.org/10.1016/j.jbiomech.2010.07.011 PMID: 20728892

27. Hansen KB, Arzani A, Shadden SC. Mechanical platelet activation potential in abdominal aortic aneurysms. J. Biomech. Eng. 2015; 137(4):041005. https://doi.org/10.1115/1.4029580 PMID: 25588057

28. Westein E, van der Meer AD, Kuijpers MJ, Frimat JP, van den Berg A, Heemskerk JW. Atherosclerotic geometries exacerbate pathological thrombus formation poststenosis in a von Willebrand factor-dependent manner. Proc. Natl. Acad. Sci. USA. 2013; 110(4):1357–62. https://doi.org/10.1073/pnas.1209905110 PMID: 23288905

29. Ramstack JM, Zuckerman L, Mockros LF. Shear-induced activation of platelets. J. Biomech. 1979; 12 (2):113–25. https://doi.org/10.1016/0021-9290(79)90150-7 PMID: 422576

30. Wurzinger LJ, Opitz R, Blasberg E, Eschweiler H, Schmid-Schönbein H. The role of hydrodynamic factors in platelet activation and thrombotic events: the effects of shear stress of short duration. In: Schettler G, Nerem RM, Schmid-Schönbein H, Mörl H, Diehm C, editors. Fluid dynamics as a localizing factor for atherosclerosis. Springer, Berlin, Heidelberg; 1983. pp. 91–102.

31. Holme PA, Ørvim U, Hamers MJ, Solum NO, Brosstad FR, Barstad RM, et al. Shear-induced platelet activation and platelet microparticle formation at blood flow conditions as in arteries with a severe stenosis. Arterioscler. Thromb. Vasc. Biol. 1997; 17(4):646–53. https://doi.org/10.1161/01.atv.17.4.646 PMID: 9108776

32. Casa LD, Ku DN. High shear thrombus formation under pulsatile and steady flow. Cardiovasc. Eng. Techn. 2014; 5(2):154–63.

33. Chen Z, Mondal NK, Ding J, Koenig SC, Slaughter MS, Wu ZJ. Paradoxical effect of nonphysiological shear stress on platelets and von Willebrand factor. Artif. Organs. 2016; 40(7):659–68. https://doi.org/10.1111/aor.12606 PMID: 26582038

34. Rahman S, Fogelson A, Hlady V. Effects of elapsed time on downstream platelet adhesion following transient exposure to elevated upstream shear forces. Colloids Surf. B Biointerfaces. 2020:111118. https://doi.org/10.1016/j.colsurfb.2020.111118 PMID: 32450503

35. Zlobina KE, Guria GT. Platelet activation risk index as a prognostic thrombosis indicator. Sci. Rep. 2016; 6:30508. https://doi.org/10.1038/srep30508 PMID: 27461235

36. Buguin A, Brochard-Wyart F. Unwinding of globular polymers under strong flows. Macromolecules. 1996; 29(14):4937–43.

37. De Gennes PG. Dynamics of a single chain. In: De Gennes PG, editor. Scaling concepts in polymer physics. Cornell University Press; 1979. pp. 165–204.

38. Arnold VI. Investigation of the equations of motion. In: Halmos PR, Gehring FW, Moore CC, editors. Mathematical methods of classical mechanics. Springer- Verlag; 1978. pp. 15–52.

39. Moake JL, Turner NA, Stathopoulos NA, Nolasco LH & Hellums JD. Involvement of large plasma von Willebrand factor (vWF) multimers and unusually large vWF forms derived from endothelial cells in shear stress-induced platelet aggregation. J. Clin. Invest. 1986; 78(6):1456–61. https://doi.org/10.1172/JCI112736 PMID: 3491092

40. Goto S, Salomon DR, Ikeda Y, Ruggeri ZM. Characterization of the unique mechanism mediating the shear-dependent binding of soluble von Willebrand factor to platelets. J. Biol. Chem. 1995; 270 (40):23352–61. https://doi.org/10.1074/jbc.270.40.23352 PMID: 7559492

41. Zhang C, Kelkar A, Neelamegham S. von Willebrand factor self-association is regulated by the shear-dependent unfolding of the A2 domain. Blood Adv. 2019; 3(7):957–68. https://doi.org/10.1182/bloodadvances.2018030122 PMID: 30936056

42. Lee H, Na W, Lee BK, Lim CS, Shin S. Recent advances in microfluidic platelet function assays: Moving microfluidics into clinical applications. Clin. Hemorheol. Microcirc. 2019; 71(2):249–66. https://doi.org/10.3233/CH-189416 PMID: 30584134

43. Tovar-Lopez FJ, Rosengarten G, Westein E, Khoshmanesh K, Jackson SP, Mitchell A, et al. A microfluidics device to monitor platelet aggregation dynamics in response to strain rate micro-gradients in flowing blood. Lab Chip. 2010; 10(3):291–302. https://doi.org/10.1039/b916757a PMID: 20091000

44. Wu WT, Zhussupbekov M, Aubry N, Antaki JF, Massoudi M. Simulation of thrombosis in a stenotic microchannel: The effects of vWF-enhanced shear activation of platelets. Int. J. Eng. Sci. 2020; 147:103206. https://doi.org/10.1016/j.ijengsci.2019.103206

45. Stockschlaeder M, Schneppenheim R, Budde U. Update on von Willebrand factor multimers: focus on high-molecular-weight multimers and their role in hemostasis. Blood Coagul. Fibrinolysis. 2014; 25 (3):206–16. https://doi.org/10.1097/MBC.0000000000000065 PMID: 24448155

46. Shadden SC, Arzani A. Lagrangian postprocessing of computational hemodynamics. Ann. Biomed. Eng. 2015; 43(1):41–58. https://doi.org/10.1007/s10439-014-1070-0 PMID: 25059889

47. Zhang JN, Bergeron AL, Yu Q, Sun C, McBride L, Bray PF, et al. Duration of exposure to high fluid shear stress is critical in shear-induced platelet activation-aggregation. Thromb. Haemost. 2003; 90 (4):672–8. https://doi.org/10.1160/TH03-03-0145 PMID: 14515188

48. Girdhar G, Bluestein D. Biological effects of dynamic shear stress in cardiovascular pathologies and devices. Expert Rev. Med. Devices. 2008; 5(2):167–81. https://doi.org/10.1586/17434440.5.2.167 PMID: 18331179

49. Yin W, Shanmugavelayudam SK, Rubenstein DA. The effect of physiologically relevant dynamic shear stress on platelet and endothelial cell activation. Thromb. Res. 2011; 127(3):235–41. https://doi.org/10.1016/j.thromres.2010.11.021 PMID: 21172720

50. Shadden SC, Hendabadi S. Potential fluid mechanic pathways of platelet activation. Biomech. Model. Mechanobiol. 2013; 12(3):467–74. https://doi.org/10.1007/s10237-012-0417-4 PMID: 22782543

51. Wellings PJ, Ku DN. Mechanisms of platelet capture under very high shear. Cardiovasc. Eng. Technol. 2012; 3(2):161–70.

52. Brass LF, Diamond SL. Transport physics and biorheology in the setting of hemostasis and thrombosis. J. Thromb. Haemost. 2016; 14(5):906–17. https://doi.org/10.1111/jth.13280 PMID: 26848552

53. Casa LD, Ku DN. Thrombus formation at high shear rates. Annu. Rev. Biomed. Eng. 2017; 19:415–33. https://doi.org/10.1146/annurev-bioeng-071516-044539 PMID: 28441034

54. Hellums JD. 1993 Whitaker Lecture: biorheology in thrombosis research. Ann. Biomed. Eng. 1994; 22 (5):445–55. https://doi.org/10.1007/BF02367081 PMID: 7825747

55. Ross R. Atherosclerosis—an inflammatory disease. N. Engl. J. Med. 1999; 340(2):115–26. https://doi.org/10.1056/NEJM199901143400207 PMID: 9887164

56. Caro CG, Pedley TJ, Schroter RC, Seed WA. Basic ideas in fluid mechanics. In: Caro CG, Pedley TJ, Schroter RC, Seed WA, editors. The Mechanics of the circulation, 2th edition. Cambridge University Press; 2012. pp. 31–44.

57. Batchelor GK. Equations governing the motion of a fluid. In: Batchelor GK, editor. An introduction to fluid dynamics. Cambridge University Press; 2000. pp. 131–73.

58. Wu WT, Yang F, Wu J, Aubry N, Massoudi M, Antaki JF. High fidelity computational simulation of thrombus formation in Thoratec HeartMate II continuous flow ventricular assist device. Sci. Rep. 2016; 6:38025. https://doi.org/10.1038/srep38025 PMID: 27905492

59. Consolo F, Sheriff J, Gorla S, Magri N, Bluestein D, Pappalardo F, et al. High frequency components of hemodynamic shear stress profiles are a major determinant of shear-mediated platelet activation in therapeutic blood recirculating devices. Sci. Rep. 2017; 7(1):4994. https://doi.org/10.1038/s41598-017-05130-5 PMID: 28694489

60. Avtaeva YN, Mel'nikov IS, Gabbasov ZA. Real-time recording of platelet adhesion to fibrinogen-coated surface under flow conditions. Bull. Exp. Biol. Med. 2018; 165(1):157–60. https://doi.org/10.1007/s10517-018-4119-5 PMID: 29796802

61. Melnikov I, Avtaeva Y, Kozlov S, Nozadze D, Gabbasov Z. P721 Shear stress induced unfolding of von willebrand factor may be involved in the premature development of myocardial infarction. Eur. Heart J. 2019; 40(Supplement_1):ehz747-0326. https://doi.org/10.1093/eurheartj/ehz747.0326

62. Lippok S, Radtke M, Obser T, Kleemeier L, Schneppenheim R, Budde U, et al. Shear-induced unfolding and enzymatic cleavage of full-length VWF multimers. Biophys. J. 2016; 110(3):545–54. https://doi.org/10.1016/j.bpj.2015.12.023 PMID: 26840720

63. Bortot M, Ashworth K, Sharifi A, Walker F, Crawford NC, Neeves KB, et al. Turbulent flow promotes cleavage of VWF (von Willebrand factor) by ADAMTS13 (a disintegrin and metalloproteinase with a thrombospondin type-1 motif, member 13). Arterioscler. Thromb. Vasc. Biol. 2019; 39(9):1831–42. https://doi.org/10.1161/ATVBAHA.119.312814 PMID: 31291760

64. Zhang P, Gao C, Zhang N, Slepian MJ, Deng Y, Bluestein D. Multiscale particle-based modeling of flowing platelets in blood plasma using dissipative particle dynamics and coarse grained molecular dynamics. Cell. Mol. Bioeng. 2014; 7(4):552–74. https://doi.org/10.1007/s12195-014-0356-5 PMID: 25530818

65. Yazdani A, Li H, Humphrey JD, Karniadakis GE. A general shear-dependent model for thrombus formation. PLoS Comput. Biol. 2017; 13(1):e1005291. https://doi.org/10.1371/journal.pcbi.1005291 PMID: 28095402

66. Fuchs G, Berg N, Broman LM, Wittberg LP. Modeling sensitivity and uncertainties in platelet activation models applied on centrifugal pumps for extracorporeal life support. Sci. Rep. 2019; 9(1):8809. https://doi.org/10.1038/s41598-019-45121-2 PMID: 31217491

67. Tsai HM. Physiologic cleavage of von Willebrand factor by a plasma protease is dependent on its conformation and requires calcium ion. Blood. 1996; 87(10):4235–44. PMID: 8639782

68. De Meyer SF, De Maeyer B, Deckmyn H, Vanhoorelbeke K. Von Willebrand factor: drug and drug target. Cardiovasc. Haematol. Disord. Drug Targets. 2009; 9(1):9–20.

69. Chen J, Reheman A, Gushiken FC, Nolasco L, Fu X, Moake JL, et al. N-acetylcysteine reduces the size and activity of von Willebrand factor in human plasma and mice. J. Clin. Invest. 2011; 121(2):593–603. https://doi.org/10.1172/JCI41062 PMID: 21266777